Scalable Computing: Practice and Experience, ISSN 1895-1767, http://www.scpe.org
© 2024 SCPE. Volume 25, Issues 6, pp. 5197–5204, DOI 10.12694/scpe.v25i6.3268

DESIGN AND SIMULATION ANALYSIS OF BRIDGE ANTI-COLLISION STRUCTURE BASED ON NONLINEAR NUMERICAL SIMULATION

RUIFANG CHEN* AND YANXIN ZHANG†

Abstract. In order to solve the dynamic nonlinear problem of bridge loads and responses during ship collisions, a design method for bridge anti-collision structures based on nonlinear numerical simulation was proposed. The author describes in detail the entire process of collision force evolution, energy conversion, and plastic deformation of the anti-collision energy dissipator, and conducts a comprehensive simulation of it. The experimental results show that when a ship with a mass of 1000 tons collides forward at speeds of 1, 3, and 5 meters per second, the collision depth is 0.23, 1.46, and 3.95 meters, respectively, less than the maximum allowable collision depth of 4.3 meters, and the collision energy dissipator is still in the protective working state for the bridge pier. When a ship with a mass of 3000 tons collides with the collision avoidance energy dissipator at a speed of 3 or 5 meters per second, the collision depth exceeds the maximum allowable collision depth, and the collision avoidance energy dissipator fails, the ship will directly collide with the wharf. The plastic deformation of the anti-collision energy dissipator provided has important reference value for design.

Key words: Ship-bridge collision, Nonlinear finite element, Anti-collision energy dissipator, Plastic deformation

1. Introduction. In recent years, with the rapid development of China's national economy, a large number of bridges across major rivers and seas are being planned, constructed or put into use. The piers of these large bridges may be accidentally hit by ships of tens of thousands of tons. The impact load is one of the important control data for bridge design. At present, there are quite a number of empirical formulas that can be used to estimate the collision force of a certain tonnage ship against the pier, but their parameters are simple and cannot describe the details of the bow structure. Unlike other engineering structural problems, the ship-bridge collision force can hardly be obtained through the scale model test, because the dynamic plastic deformation of the bow structure occurs during the collision, and the similarity law cannot be established for this strong nonlinear mechanical process at present. Therefore, using modern nonlinear finite element technology and software, through the numerical simulation of the collision process, is the best and most accurate method to obtain the ship-bridge collision load at present [1,2].

Ship-bridge collision is a different process involving non-uniformity, geometric nonlinearity, contact nonlinearity and other phenomena, so it is difficult to conduct theoretical research on it. However, the cost of comprehensive research is very high, and research conclusions are limited by experimental technology; It is difficult to accommodate many nonlinear factors in a measurement system. Existing research on ship-bridge collisions is mainly based on experimental methods, focusing on the effects of ship-bridge collision forces, flow process corrections, and basic structures of collision structures.

With the rapid development of water transportation in China, the number of newly-built bridges has gradually increased, but the ship-bridge collision accidents have also become more frequent, resulting in major losses such as bridge damage and collapse, channel obstruction, threat to people's lives and property, and environmental pollution. Therefore, the study of ship collision force of bridges is particularly important [3,4], as shown in Figure 1.1.

2. Literature review. The existing research shows that when the bow collides with the pier of a large bridge, the pier stiffness is far greater than the structural stiffness of the bow. The main aspect of damage is the bow. The collision force and its time history are mainly determined by the collapse strength of the bow structure. When the bow strikes the plane part of a large pier, the pier can be simplified as a rigid plane wall.

*School of Architecture and Engineering, City University of Zhengzhou, China (Corresponding author, RuifangChen9@163.com)
†College of Water Conservancy and Civil Engineering, Zhengzhou University, China (YanxinZhang7@126.com)

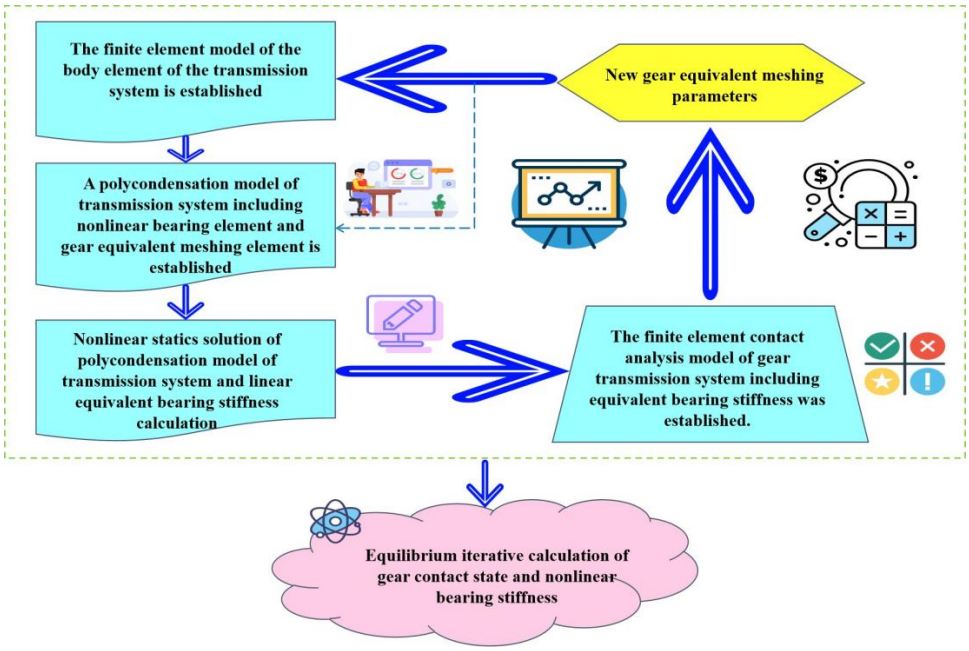

Fig. 1.1: Bridge anti-collision structure of nonlinear numerical simulation

Based on this, we can calculate the collision force of bow and rigid wall of various tonnage ships in advance, which is very close to the collision force of real ship and real bridge, for reference of bridge design. However, for different ships of the same tonnage, the rigidity of the bow structure is not the same, so the collision force of the ship bridge is also different, but generally in a close range [5,6].

Minorsky theory, Hans Drucher theory and simplified analytical method are the basis of commonly used methods for analyzing ship-bridge collision problems nowadays, but the above theories are based on quasi-static simulation analysis of collision. However, ship-bridge collision is a complex nonlinear dynamic response process of bridge structure and hull structure under huge impact load in a short time. It has very obvious dynamic characteristics, and the components in the collision zone generally need to quickly surpass the elastic stage and enter the plastic stage, and may have various forms of damage such as tearing and buckling, so it is not accurate to analyze the ship-bridge collision with the existing ship-bridge collision theory [7].

With the increasing progress and maturity of nonlinear finite element technology, it is widely used in the numerical simulation of structural impact, making the finite element numerical simulation technology can better solve the ship-bridge collision problem. Based on the basic theory and key technology of collision simulation, this paper numerically simulates the forward collision process of a ship's anti-collision energy dissipator on the main bridge pier of a bridge. We also describe and analyze the collision force evolution, collision energy conversion and collision avoidance capability (i.e. maximum absorbed energy) of collision energy dissipator during the collision process, and study the inherent regularity of collision phenomenon. It shows the advantages and prospects of the application of collision numerical simulation analysis.

3. Methods.

3.1. Nonlinear finite element control equation. The equation of motion of the ship-bridge collision problem can be generally expressed as

$$[M]\{\ddot{d}\} + [C]\{\dot{d}\} + [K]\{d\} = \{F^{ex}\} \tag{3.1}$$

where $[M]$ is the bridge mass matrix; $[C]$ is the damping matrix; $[K]$ is the stiffness matrix; $\{\ddot{d}\}$ is the acceleration vector; $\{d\}$ is the velocity vector; $\{d\}$ is the displacement vector; $\{F^{ex}\}$ is the external force vector. The

collision force is output in the form of contact force by defining the ship/collision avoidance system as the contact surface[8,9].

The explicit direct time domain integration method is suitable for the transient dynamic problems formed after the finite element discretization. By automatically controlling the time step, we can obtain a stable solution and ensure the accuracy of time integration. In practice, the minimum time step is defined by dividing the characteristic length of the minimum finite element mesh by the stress wave velocity:

$$\Delta t \leqslant \Delta t_{cr} = min(L^e/C) \tag{3.2}$$

3.2. Contact algorithm in collision. Collision-style (or composite) interaction is performed by the contact algorithm. A master-slave contact surface is defined between two contacting surfaces. Check if the slave has access to the main interface at any point in the resolve. Otherwise, the calculation will continue; Otherwise, a shearing force is applied to the base face to prevent the slave from further penetrating, and this force is the contact force [10].

The calculation in this paper is completed with the help of the powerful nonlinear finite element software LS-DYNA.

3.3. Project overview of collision simulation calculation model between ship and anti-collision energy dissipator. A bridge is a PC continuous rigid frame bridge. The main pier is a double-thin-walled pier. The size of the foundation cap is 18.6mx12.6mx5m. The design requires navigation of ships with a full load of 1000t. The main pier of the bridge is equipped with anti-collision energy dissipator in the form of angle steel supporting steel pipe frame. The material is Q235 steel, the diameter of steel pipe is 800 mm, the thickness is 10 mm, the model of support angle steel is 100 mm x 100 mm x 10 mm, and the thickness of node steel plate is 10 mm except for 1 6, which is 20 mm [11].

3.4. Strain rate sensitivity analysis of materials. At the same time, most of the anti-collision bridges are made of low carbon. The plastic material of the steel material is sensitive to the filter value, and its strength increases with the filter value. Therefore, the effect of different costs of intervention should be included in the model used to determine the difference in the problem. Among the constitutive equations that understand the components, the Cowper-Symonds constitutive equation is the most widely accepted.

$$\sigma_0'/\sigma_0 = 1 + (\varepsilon'/D)^{1/q} \tag{3.3}$$

where σ_0' is the dynamic yield stress at plastic strain rate ε'; σ_0 is the corresponding static yield stress; D and q are the strain rate parameters of the material. For mild steel, D=40.4, q=5.

For the steel used for anti-collision device, the contribution of isotropic strengthening and follow-up strengthening to the material needs to be included in the strengthening parameter β. $\beta = 0$ for follow-up strengthening and $\beta = 1$ for isotropic strengthening. Therefore, the improved Cowper-Symonds constitutive equation is adopted for the anti-collision device in the analysis of ship collision bridge problems

$$\sigma_0' = [1 + (\varepsilon'/D)^{1/q}](\sigma_0 + \beta E_p \varepsilon_p^{eff}) \tag{3.4}$$

where E_p is the plastic strengthening modulus; ε_p^{eff} is the effective plastic strain.

3.5. Establishment of finite element model for numerical simulation analysis. The collision process of ships and bridge structures is highly dependent on environmental conditions (wind, waves, weather, water, etc.) and ship characteristics (ship type, size, speed, load, bow force, stiffness). is complicated., hull and deck house, etc.), bridge characteristics (size, shape, material, quality, bridge characteristics, etc.) and steering response time. Due to the complexity of the ship-bridge collision process, it needs to be simplified in numerical simulation analysis. In the study of ship bridge collisions, the ship's rotational forces and the relationship between the ship's bridge and the bridge structure are important [12,13,14].

The key to study the anti-collision energy dissipation effect of the anti-collision energy dissipator of bridge structure is to obtain the impact force between ships and bridges and the energy absorption of the anti-collision energy dissipator during the impact process. Therefore, the finite element model of the anti-collision energy dissipator is only established when studying the anti-collision energy dissipator. Since the dynamic response of

the upper and lower structures of the bridge has little impact on the energy transfer and absorption, it can be ignored [15].

The water medium around the hull moves with the hull and participates in the absorption of collision energy. Since the hull is mainly rigidly displaced longitudinally in the collision when the ship collides with the anti-collision structure, the impact of the water medium around it is relatively small. The impact of water can be fairly accurately expressed by using an additional water mass 0.04 times the total mass of the hull.

In the study of collision between ships and anti-collision structures, it is very important to establish an effective finite element model in numerical simulation. When establishing the finite element model of anti-collision structure, because the joint steel plates between angle steel and angle steel and between angle steel and steel pipe are relatively rigid, rigid joints are used in the finite element model, and fixed bearings are used at the connection of angle steel support and foundation bearing platform; Since the deformation energy absorption capacity of anti-collision energy dissipator is mainly studied during the collision process, it is reasonable to use beam element to simulate steel pipe and angle steel support in DY-NA program. The section of steel pipe beam element and angle steel beam element are hollow steel pipe section and angle steel section respectively, and the finite element model of anti-collision energy dissipator.

When a ship collides with an anti-collision structure, the energy in the collision process mainly comes from the rotational forces of the ship. After the collision, the anti-collision force will absorb most of the energy, and the body will undergo some deformation to absorb some of the energy. In finite element modeling of the ship, shell material (THIN SHELL163 element) is used for the contact between the ship collision and the damage of the anti-collision structure to simulate the deformation of the ship during the collision. e.g. bow), stabilizers are used to change the accuracy of the ship (including additional water) and to ensure that the ship's torque during collisions is consistent with the truth. Deformation of the ship affects only the deformation of the hull falling on the bow [16].

Based on the above discussion, the LS-DYNA nonlinear finite element program is used to establish the finite element model of the anti-collision energy dissipator and the ship of a bridge, and the forward collision process between the ship and the anti-collision energy dissipator is numerically simulated, and the dynamic performance of the anti-collision energy dissipator during the collision process is studied. In the numerical simulation analysis, the beam element (BEAM161) is used to simulate the anti-collision structure. The ship uses two types of shell element (SHELL163) and solid element (SOL-ID164). In the whole finite element model, there are 16240 beam elements, 25000 shell elements and 500 solid elements.

For marine low-carbon steel and anti-collision structural low-carbon steel, the material has entered the nonlinear stage during the collision. The bilinear strengthening elastoplastic constitutive relation is adopted for low-carbon steel materials, and the improved Cowper-Symonds constitutive equation is adopted for material properties. In the material, only the contribution of follow-up strengthening to low carbon steel is considered. The values of parameters in the calculation model are as follows: material density $\rho = 7.85 \times 10^3 kg/m^3$, elastic modulus $E = 2.1 \times 10^{11} N/m^2$, hardening modulus $E_h = 1.18 \times 10^9 N/m^2$, yield stress $\sigma_0 = 2.35 \times 10^8 N/m^2$, Poisson's ratio $v = 0.3$, strain rate parameter D=40.4, strain rate parameter q=5, hardening parameter $\beta = 0$, maximum failure and other effects $\varepsilon_{failure} = 0.34$.

4. Results and discussion.

4.1. Collision force analysis between ship and anti-collision structure. The collision force between the ship and the anti-collision structure refers to the interaction force (i.e. the contact force between the two) when they collide. The size of the collision force represents the degree of damage of the ship to the anti-collision structure.

Figure 4.1 shows the time-history curve of the collision force between the ship and the anti-collision structure during the forward collision of a 1000t ship with the anti-collision energy dissipator at a speed of 3 m/s. It can be seen from the figure that the impact force curve has nonlinear wave characteristics. At different stages of the collision process, the collision force jumps to different degrees. Each jump increase of the collision force indicates that the propagation of the stress wave makes some components in the anti-collision structure effectively participate in the anti-collision work; The jump reduction of each collision force indicates the failure or failure of some components. In this example, the drop of impact force is mainly caused by the dynamic buckling of some angle steel supporting frame structures [17,18].

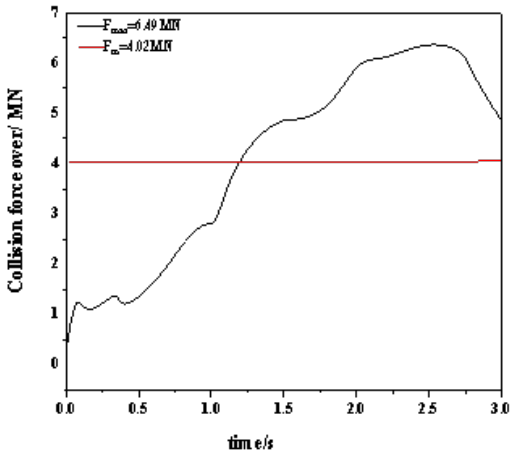

Fig. 4.1: Time history curve of impact force

In Figure 4.1, $F_{max} = 6.49MN$ represents the maximum collision force in the collision process, and represents the average collision force in the collision process. It can be seen from the figure that at the beginning, the collision force gradually increases with the increase of time (that is, the increase of impact depth). When the maximum collision force occurs, the collision force curve starts to slide (that is, the last section of the collision force curve). This is due to the rebound of the ship after the collision with the anti-collision structure. The above calculation results are basically consistent with the existing research results.

Table 4.1 lists collisions between 1000t and 3000t ships in head-on collisions with anti-collision energy dissipators at speeds of 1, 3, and 5 m/s. During a collision, the maximum force of the collision is very large, but the duration is short, so the damage to the structure is very small. Therefore, the collision damage of ships and anti-collision energy emitters of bridge structures are mainly determined by the size of the middle part of the collision force of the connection, that is, the greater the average collision force during the collision, the greater the energy emitter from the collision damage to prevent the collision. As the table shows, the force of the boat increases at the beginning of the turn, and the average collision force also increases. It can be concluded that the greater the ship's turning force, the greater the average collision force and the greater the effect of the collision force dissipator. From the ratio of the average collision force to the maximum collision force, it is not difficult to see that the average collision force is about half of the maximum collision force, which is consistent with the conclusion that the maximum collision force is twice the average. The force of the collision as demonstrated by the results of the Warsing experiment [19].

4.2. Energy conversion during collision. During the collision, the initial collision kinetic energy of the ship (including the kinetic energy provided by the additional water mass) will be converted into the following energy: the elastic-plastic deformation energy and the residual kinetic energy of the collision ship; Elastoplastic deformation energy and kinetic energy of anti-collision structure; Thermal damage caused by friction between components. In addition, the volume element and shell element in DY-NA program have only one integral point (located at the centroid of the element). Some deformation modes of the element do not have stiffness, resulting in the hourglass phenomenon and causing certain energy loss. The energy loss caused by the hourglass can be controlled to a small amount by adding viscous damping coefficient and reasonably dividing the grid. The calculation results show that the energy loss caused by friction is very small in the above energy. Therefore, the initial kinetic energy of the ship is mainly converted into the deformation energy and kinetic energy of the anti-collision structure, and the deformation energy and residual kinetic energy of the collision ship.

Figure 4.2 shows the energy conversion and energy time history curves for collision avoidance, and the

Table 4.1: Comparison of collision forces when ships with different initial kinetic energy collide with anti-collision energy dissipators in the forward direction

Ship mass/t	Initial velocity of collision/(m/s)	Collision initial Kinetic energy/MJ	Maximum impact force (F_{max})/MN	Average collision force (F_m)/MN	$\eta = F_m/F_{max}/\%$
1000	1	0.5	3.23	1.82	56.3
	3	4.5	6.49	4.02	61.9
	5	12.5	8.35	5.02	60.1
3000	1	1.5	4.54	2.43	53.5
	3	13.5	9.67	5.90	61.0
	5	37.5	11.35	6.53	57.5

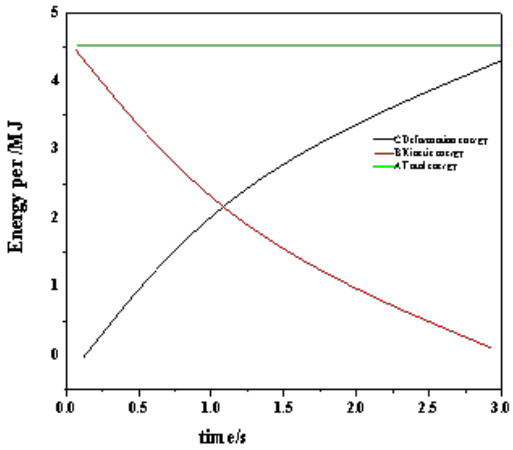

Fig. 4.2: Energy time-history curve

electrical energy of a 1000-ton ship when the next ship collides with a speed of 3 m/s. Line A represents the total energy of the entire system, while lines B and C represent the rotational energy and deformation energy of the entire system (rotational energy and deformation energy of the entire system, including the collision avoidance installation and the ship). As you can see from the figure, the bending force of the whole system (line B) is gradually decreasing, while the deformation energy of the whole system (line C) is gradually increasing, so yes, the rotational energy of the system is changing. the deformation energy of the system, but the total energy of the whole system (line A) remains unchanged (line A is horizontal), - this only shows that the transformation of energy in the collision process is consistent with the law of conservation of energy.

4.3. Damage and deformation analysis of anti-collision energy dissipator. Under the impact of ships with different initial kinetic energy, the size of the plastic deformation of the anti-collision energy dissipator of the pier is different. When its plastic deformation is greater than the safe design distance (i.e. the maximum allowable impact depth), the anti-collision energy dissipator will fail and the ship will directly impact the pier. Therefore, in the numerical simulation analysis, it is specified that when the ship directly collides and contacts the pier surface, the anti-collision energy dissipator will exit the protective working state. The maximum allowable impact depth of anti-collision energy dissipator is 4.3m[20].

Table 4.2 lists the deformation energy and impact depth of 1000t and 3000t ships when they collide with the anti-collision energy dissipator at the speed of 1, 3 and 5 m/s. It can be seen from the table that when the

Table 4.2: Deformation energy and impact depth of anti-collision energy dissipator under forward collision of ships with different initial kinetic energy

Ship mass /t	Initial velocity of collision /(m/s)	Initial kinetic energy of collision /MJ	Kinetic energy at the end of collision /MJ	Deformation energy of anti-collision energy dissipator /MJ	Impact depth /m	Whether the anti-collision energy dissipator fails
1000	1	0.5	0.12	0.30	0.23	No
	3	4.5	0.78	3.49	1.46	No
	5	12.5	0.71	11.45	3.95	No
3000	1	1.5	0.33	1.05	0.72	No
	3	13.5	0.37	12.77	4.30	Yes
	5	37.5	24.10	13.03	4.30	Yes

ship collides with the anti-collision energy dissipator, most of the dissipated kinetic energy is converted into the deformation energy of the anti-collision energy dissipator (that is, absorbed by the anti-collision structure). As the initial kinetic energy of the ship increases, the impact depth of the anti-collision energy dissipator also increases. When a ship with a mass of 1000 tons collides with the anti-collision energy dissipator in the forward direction at the speed of 1, 3 and 5 m/s, the impact depth is 0.23, 1.46 and 3.95 m respectively, which are less than the maximum allowable impact depth of 4.3 m, and the anti-collision energy dissipator is still in the protective working state for the pier.

When a ship with a mass of 3000t collides with the anti-collision energy dissipator in the forward direction at a speed of 3 or 5m/s, the impact depth exceeds the maximum allowable impact depth, the anti-collision energy dissipator has failed, and the ship will directly hit the pier. It is not difficult to find from the table that the anti-collision capacity (i.e. the maximum absorbed energy) of the anti-collision energy dissipator is only related to its own structure and material properties, but not to the initial kinetic energy of the collision ship.

5. Conclusion. This paper presents the design and simulation analysis of bridge anti-collision structure based on nonlinear numerical simulation. This method uses explicit transient nonlinear finite element analysis technology to successfully simulate the collision process of ship and bridge structure anti-collision energy dissipator. The results of numerical simulation analysis can reflect the general phenomena and basic laws in the collision process, and can more accurately reproduce the dynamic process inside the structure. The simulation analysis results can also simulate and reproduce the whole time course of collision force evolution, energy conversion and plastic deformation of anti-collision structure in the process of collision between ships and anti-collision energy dissipators.

REFERENCES

[1] Rao, X., Xu, Y., Liu, D., Liu, Y., & Hu, Y. (2021). A general physics-based data-driven framework for numerical simulation and history matching of reservoirs. Advances in Geo-Energy Research, 5(4), 422-436.
[2] Gelin, M., & Borrelli, R. (2021). Simulation of nonlinear femtosecond signals at finite temperature via a thermo field dynamics-tensor train method: general theory and application to time- and frequency-resolved fluorescence of the fenna-matthews-olson complex. Journal of chemical theory and computation, 17(7), 4316-4331.
[3] Ding, J., Yin, W., & Ma, Y. (2021). Large eddy simulation and flow field analysis of car on the bridge under turbulent crosswind. Mathematical Problems in Engineering, 2021(2), 1-10.
[4] Chang, X., & Sharma, A. (2021). Analysis and design of general bridge crane structure using cad technology. Computer-Aided Design and Applications, 19(S2), 15-25.
[5] Xiao, X., Xue, H., & Chen, B. (2021). Nonlinear model for the dynamic analysis of a time-dependent vehicle-cableway bridge system. Applied Mathematical Modelling, 90(1-2), 1049-1068.
[6] Han, D., Xu, L., Cao, R., Gao, H., & Lu, Y. (2021). Anti-collision voting based on bluetooth low energy improvement for the ultra-dense edge. IEEE Access, PP(99), 1-1.
[7] Xing, X., Lin, L., & Qin, H. (2021). An efficient cable-type energy dissipation device for prevention of unseating of bridge spans. Structures, 32(1), 2088-2102.

[8] Wany, M., Falkowski, K., Wrblewski, M., Wojtowicz, K., & Marut, A. (2021). Conceptual design of an anti-collision system for light rail vehicles. Problems of Mechatronics Armament Aviation Safety Engineering, 12(1), 9-26.
[9] Patrucco, M., Pira, E., Pentimalli, S., Nebbia, R., & Sorlini, A. (2021). Anti-collision systems in tunneling to improve effectiveness and safety in a system-quality approach: a review of the state of the art. Infrastructures, 6(3), 42.
[10] Ma, R. (2021). Analysis and design based on the operation mode of power electronic transformer in smart grid. Journal of Physics: Conference Series, 2108(1), 012073-.
[11] Hegendrfer, A., Steinmann, P., & Mergheim, J. (2022). Nonlinear finite element system simulation of piezoelectric vibration-based energy harvesters:. Journal of Intelligent Material Systems and Structures, 33(10), 1292-1307.
[12] Zhang, L., Xie, Z., Li, J., Zhang, J., Yu, Q., & Zhang, C. (2022). A new polyurethane-steel honeycomb composite pier anti-collision device: concept and compressive behavior:. Advances in Structural Engineering, 25(4), 820-836.
[13] Lu, K., Chen, X. J., Gao, Z., Cheng, L. Y., & Wu, G. H. (2021). Initial response mechanism and local contact stiffness analysis of the floating two-stage buffer collision-prevention system under ship colliding:. Advances in Structural Engineering, 24(10), 2227-2241.
[14] Pandey, N., Joshi, S., & Mallik, R. K. (2021). Characterizing the probability of collision between information particles in molecular communications. IEEE Wireless Communication Letters, PP(99), 1-1.
[15] Zhou, L., Zong, Z., & Li, J. N. (2022). A numerical study of hydrodynamic influence on collision of brash ice with a structural plate. Journal of Hydrodynamics, 34(1), 43-51.
[16] Pan, M., Li, X., Xie, D., & Zhao, C. (2021). Design and research of photovoltaic modules in energy routers based on cascaded h-bridge. Journal of Physics: Conference Series, 1948(1), 012157-.
[17] Birsan, M. (2021). Simulation of a ship's deperming process using the jiles–atherton model. IEEE Transactions on Magnetics, PP(99), 1-1.
[18] Maaroof, H. S., Al-Badrani, H., & Younis, A. T. (2021). Design and simulation of cascaded h-bridge 5-level inverter for grid connection system based on multi-carrier pwm technique. IOP Conference Series Materials Science and Engineering, 1152(1), 012034.
[19] Guo, W., Zhao, Q. S., Tian, Y. K., & Zhang, W. C. (2021). The research on floe ice force acting on the "xue long" icebreaker based on synthetic ice test and virtual mass numerical method. Journal of Hydrodynamics, 33(2), 271-281.
[20] Pei, L., Chen, W., Zhang, Q., Xu, M., Huang, L., & Guo, C., et al. (2022). The design and optimization of ship cabin space layout based on crowd simulation. Journal of Computer-Aided Design & Computer Graphics, 33(9), 1337-1348.

Edited by: Bradha Madhavan
Special issue on: High-performance Computing Algorithms for Material Sciences
Received: Jan 30, 2024
Accepted: Apr 4, 2024